applied sciences

MDPI

Article

Activity Concentrations of Cs-137, Sr-90, Am-241, Pu-238, and Pu-239+240 and an Assessment of Pollution Sources Based on Isotopic Ratio Calculations and the HYSPLIT Model in Tundra Landscapes (Subarctic Zone of Russia)

Andrey Puchkov and Evgeny Yakovlev *

N. Laverov Federal Center for Integrated Arctic Research f Ural Branch of the Russian Academy of Sciences, 109 Severnoj Dviny Emb., 163000 Arkhangelsk, Russia; andrey.puchkov@fciarctic.ru

* Correspondence: evgeny.yakovlev@fciarctic.ru; Tel.: +7-911-572-22-54; Fax: +7-8182-28-76-36

Abstract: The paper is devoted to the assessment of the content of anthropogenic radionuclides in tundra landscapes of the subarctic zone of Russia. The authors of the article studied the features of accumulation and migration of anthropogenic radionuclides and identified probable sources of their entry into environmental objects. Peat samples were collected on the territory of the Kaninskaya Tundra of the Nenets Autonomous Okrug (Northwest Russia). A total of 46 samples were taken. The following parameters were determined in each peat sample: (1) activity and pollution density of anthropogenic radionuclides; (2) isotopic ratios of anthropogenic radionuclides; (3) activity ratios of each radionuclide for layers 10–20 cm and 0–10 cm. The results of the studies showed that the pollution density of the Nes River basin with the radionuclides Cs-137 and Sr-90 is up to 4.85×10^3 Bq×m^{-2} and 1.88×10^3 Bq×m^{-2}, respectively, which is 2–5 times higher than the available data for the Kanin tundra, as well as for Russia and the world as a whole. The data obtained for Am-241, Pu-238, and Pu-239+240 showed insignificant activity of these radionuclides and generally correspond to the values for other tundra areas in Russia and the world. It was found that some tundra areas ("peat lowlands") are characterized by increased radionuclide content due to the process of accumulation and migration along the vertical profile. Calculations of isotope ratios Sr-90/Cs-137, Pu-238/Pu-239+240, Pu-239+240/Cs-137, Am-241/Pu-239+240 and air mass trajectories based on the HYSPLIT model showed that the main sources of anthropogenic radionuclide contamination are global atmospheric fallout and the Chernobyl accident.

Keywords: arctic; anthropogenic radionuclides; migration; accumulation; isotopic ratios; pollution sources

Citation: Puchkov, A.; Yakovlev, E. Activity Concentrations of Cs-137, Sr-90, Am-241, Pu-238, and Pu-239+240 and an Assessment of Pollution Sources Based on Isotopic Ratio Calculations and the HYSPLIT Model in Tundra Landscapes (Subarctic Zone of Russia). *Appl. Sci.* **2023**, *13*, 12952. https://doi.org/10.3390/app132312952

Academic Editor: Mauro Marini

Received: 29 October 2023
Revised: 27 November 2023
Accepted: 30 November 2023
Published: 4 December 2023

1. Introduction

In recent years, the Arctic has become one of the focal points of the global scientific community in terms of assessing the environmental risks associated with the development of its natural resources, which often results in the pollution of environmental objects with various pollutants [1–10]. In the arctic and subarctic areas of Russia, radioactive pollution is a significant factor among the many environmental problems [11,12]. For example, the northwestern sector of the Russian subarctic region is characterized by a significant number of radiation-hazardous sites, both active and with the status of "nuclear heritage sites" [13,14], the most important of which are radioactive fallout from nuclear tests, including on the Novaya Zemlya archipelago, pollution from Western European radiochemical plants in the UK and France, the consequences of the 1986 Chernobyl disaster, the activities of nuclear shipbuilding and ship repair enterprises, nuclear ship and submarine bases, and the activities of nuclear power plants and submarines [13,15–21].

The vast ecosystems of the Russian subarctic mainland are tundra, which have a significant impact on regulating the planet's climate and biogeochemical and hydrological

cycles [22,23]. Tundra is highly susceptible to human impacts. One of the primary objects of natural interest in tundra areas is the peat deposit, which represents a valuable and important archive of the level of radioactive pollution due to the fact that moss, lichen, and peat effectively trap and accumulate the pollutants that come with the atmospheric air and fallout [23]. The complex of anthropogenic radionuclides contained in peat, their activities and dose levels, as well as isotopic ratios, can be effectively used to assess the radioecological situation in the study area [24]. Sr-90/Cs-137, Pu-238/Pu-239+240, Pu-239+240/Cs-137, and Am-241/Pu-239+240 are the commonly applied technogenic isotopic ratios for the identification of radioactive pollution sources [23,25–30]. This is because of their nuclear physical and chemical properties and their role as the primary fragments and decay products following a nuclear explosion or incident [3,31].

Tundra ecosystems are prevalent in the Nenets Autonomous Okrug of the western sector in the Russian subarctic. Some nuclear heritage sites, which resulted from peaceful nuclear explosions, could pose potential risks. Examples include "Pyrite" in the Nenets Autonomous Okrug, "Agat" in the Arkhangelsk Oblast, and "Globus-3", "Globus-4", "Quartz-2", and "Horizont-1" in the Komi Republic. It is important to acknowledge the potential dangers of these sites in order to mitigate any risks they might pose in the future [32,33]. Limited information is available regarding radionuclide distribution in the tundra regions of the Nenets Autonomous Okrug. Prior investigations have revealed the existence of areas with elevated levels of anthropogenic radionuclides Cs-137 and Sr-90 in environmental objects [34–37]. In conditions of a significant number and variety of radiation-hazardous objects on the territory of Nenets Autonomous Okrug, as well as the presence of zones of increased content of anthropogenic radionuclides, it becomes relevant to assess the behavior of radionuclides in natural objects, as well as to identify the sources of their entry into the environment.

Thus, this study aims to evaluate the levels of anthropogenic radionuclides in peat from tundra regions. Additionally, it aims to analyze the accumulation and migration patterns of these radionuclides and to identify the sources of radioactive pollution based on the calculation of isotope ratios and the calculation of air mass trajectories using the HYSPLIT model (in the Nenets Autonomous Okrug, Northwestern Russian Subarctic).

2. Materials and Methods

The migration and accumulation of anthropogenic radionuclides were studied in the western region of the Nenets Autonomous Okrug, Northwest Russia, in June 2022. A total of 46 peat samples were collected along a profile with a total length of about 20 km, perpendicular to the bed of the Nes River and extending from flat peat bogs in the southwest to a local watershed in the northeast. The selection of this area was based on the findings obtained earlier, which suggest that there is a probable zone of elevated levels of anthropogenic radionuclides in environmental objects [34–37]. The activity and density of pollution with radionuclides Cs-137, Sr-90, Am-241, Pu-238, Pu-238+239, and the isotopic ratios of Sr-90/Cs-137, Pu-238/Pu-239+240, Pu-239+240/Cs-137, and Am-241/Pu-239+240 were determined in each peat sample, alongside the isotopic ratios of each radionuclide by layers 0–10 cm and 10–20 cm. The sampling profile scheme is illustrated in Figure 1. The angular coordinates of the site are as follows: N 66°30′55.9969″ E 44°28′13.8301″, N 66°40′45.7128″ E 44°28′53.3809″, N 66°40′45.7128″ E 44°54′08.6702″, N 66°31′08.8155″ E 44°54′13.6140″.

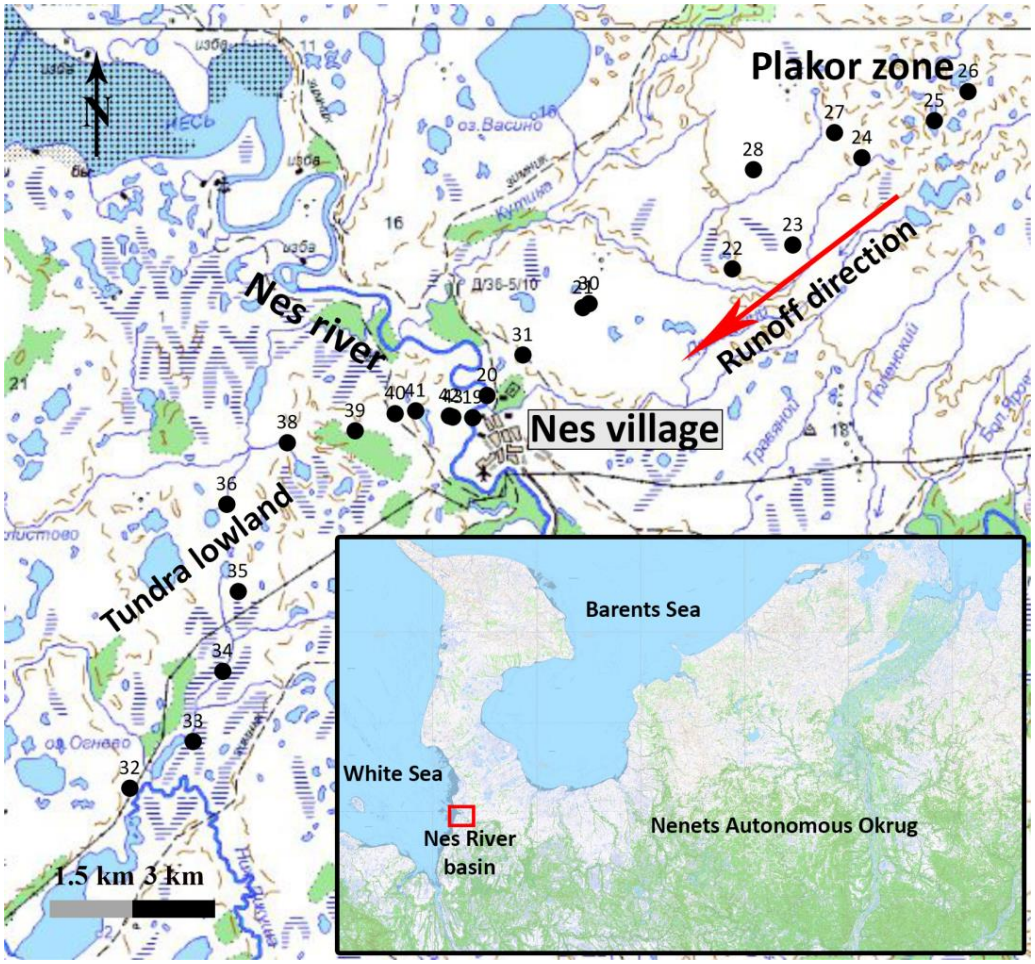

Figure 1. Scheme of the study area in the Nes River basin (Kaninskaya tundra of the Nenets Autonomous Okrug).

To comprehend the patterns of radionuclide distribution in different types of elemental landscapes, the results of the pollution density calculations for each investigated radionuclide were plotted on the elevation diagram along the sampling route (Figure 2). The altitude diagram was developed as per the results of terrain digitization using the free and open-source cross-platform desktop Geographic Information System application QGIS.

Field studies enabled the detailed characterization of the landscape of the Nes River basin. During the sampling route to the northeast of Nes (on the right bank of the river), shallow boggy peat bogs with a low moisture content were discovered (Figure 2). The cracking of the hillock surface was noted in the plakor zone and across most of the slope, an indicator of decreasing moisture content in these elementary landscapes. An elevation in wetness levels was observed as the river floodplain neared. A distinct contrast was noted on the southwestern side of Nes village, situated on the left bank of the Nes River. The terrain displayed shallow bogs with a significantly higher degree of wetness (Figure 2). High levels of peat wetness due to surface water were observed at all sampling sites. One of the reasons for these differences in the catchment area is the different types of landscape. This, in turn, affects the migration of elements, including radioactive elements. [38–42].

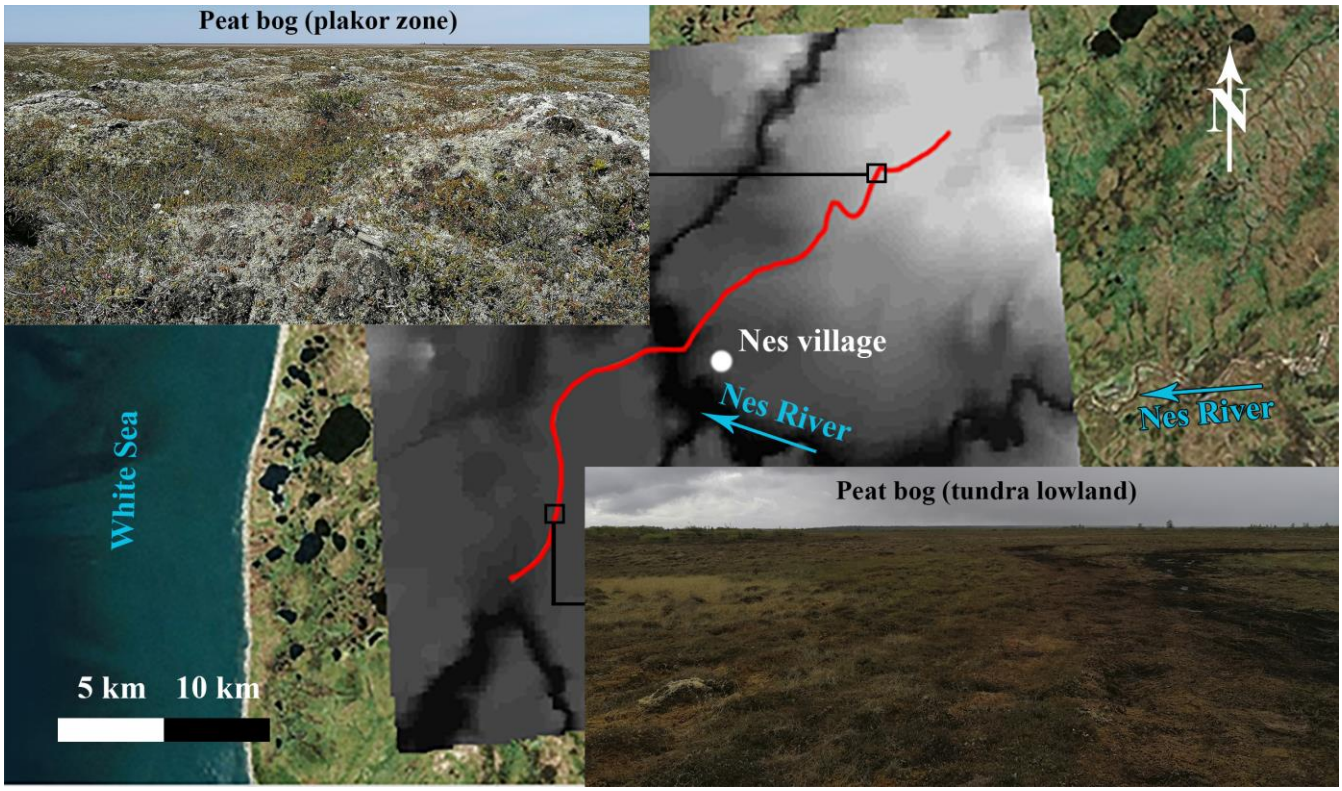

Figure 2. Digital elevation model of the Nes River basin and shallow bogs in different types of elementary landscapes.

Methods

Peat samples were taken on a 20 × 20 cm plot in 0–10 cm and 10–20 cm layers. Sample preparation, radiochemical preparation, and measurements were carried out at the Environmental Radiology Laboratory of the Federal Research Centre for Integrated Arctic Research in Arkhangelsk. The selected samples were brought to dryness in a BINDER E28 desiccator (BINDER GmbH, Tuttlingen, Germany) at 105 °C. After drying, the soil and peat samples were ashed at a temperature not exceeding 400 °C to avoid loss of radionuclides.

The levels of radionuclides Cs-137 and Am-241 were assessed using a low-background semiconductor gamma spectrometer, ORTEC (Atlanta, GA, USA), equipped with a coaxial detector GEM40. The detector was constructed using extremely pure germanium (HPGe) and SpectraLine software (version: 1.5.5396, https://www.lsrm.ru/, 2 January 2021). A resolution of 1.75 keV was reached along the 1.33 MeV (Co-60) line, and the relative efficiency was 43%. Plastic beakers of varying volumes were selected to determine the activity. The duration of measurement was selected between 2 to 5 h based on the detector loading. Additionally, it was ensured that uncertainties of the photopeak areas at 59.54 keV and 661.66 keV did not exceed 5%. The activity of radionuclide Cs-137 was calculated using the gamma line 661.66 with a quantum yield of 89.90%. The activity of radionuclide Am-241 was calculated using gamma line 59.54 keV with a quantum yield of 35.90%.

The activity of the radionuclide Sr-90 was assessed through its decay product, Y-90. The activity of Sr-90 was calculated from the measurement of Y-90 separated by radiochemical methods using the following formula:

$$A_{sr90} = \frac{N_s - N_b}{Eff \times M \times ChLos \times K_{abs}} \quad (1)$$

where A_{sr90}—Sr-90 activity in the sample, Bq×kg^{-1}; *Ns*—sample count rate on the radiometer, count per second; *Nb*—background count rate on the radiometer, count per second; *Eff*—beta-radiation energy efficiency indicator of the radiometer Y-90 (E = 2260 keV), %;

M—mass of counting sample, kg; *ChLos*—radiochemical yield of Y-90, %; *Kabs*—beta absorption coefficient, %. After radiochemical preparation, Sr-90 was determined using an alpha-beta radiometer RKS-01 Abelia (NTC Amplitude, Moscow, Russia) and a 10-channel alpha-beta radiometer LB 770 (Berthold Technologies GmbH & Co., KG, Bad Wildbad, Germany).

Plutonium isotope determination was performed following its radiochemical preparation, which included transferring radionuclides from the sample to the solution, extracting plutonium isotopes and separating them from the matrix and interfering alpha-emitting radionuclides, and electrolytic preparation of the counting sample.

Radiochemical purification involves extracting and separating plutonium isotopes from interfering alpha-emitters and macrocomponents, followed by electrolytic precipitation. A solution consisting of 30% tributyl phosphate (TBP) in toluene is used as the extractant. Chromatographic purification is carried out using anionite AB-17-8.

Following the radiochemical preparation, plutonium isotope activity was determined with an alpha-radiation energy spectrometer SEA-13P1 (NTC Aspect, Moscow, Russia).

The pollution densities of anthropogenic radionuclides were determined by accounting for both the sampling area and the total mass of the sample.

The main measured unit in this paper is the pollution density expressed in $Ci \times km^{-2}$ and $Bq \times m^{-2}$ units. We have chosen to use the unit $Ci \times km^{-2}$ for ease of comparison with the existing data on pollution in Russia.

3. Results and Discussion

3.1. Spatial Distribution of Anthropogenic Radionuclides

Figures 3 and 4 illustrate the variation in pollution density of Cs-137 and Sr-90 along the peat sampling profile. Pollution density is shown for the 0–20 cm layer.

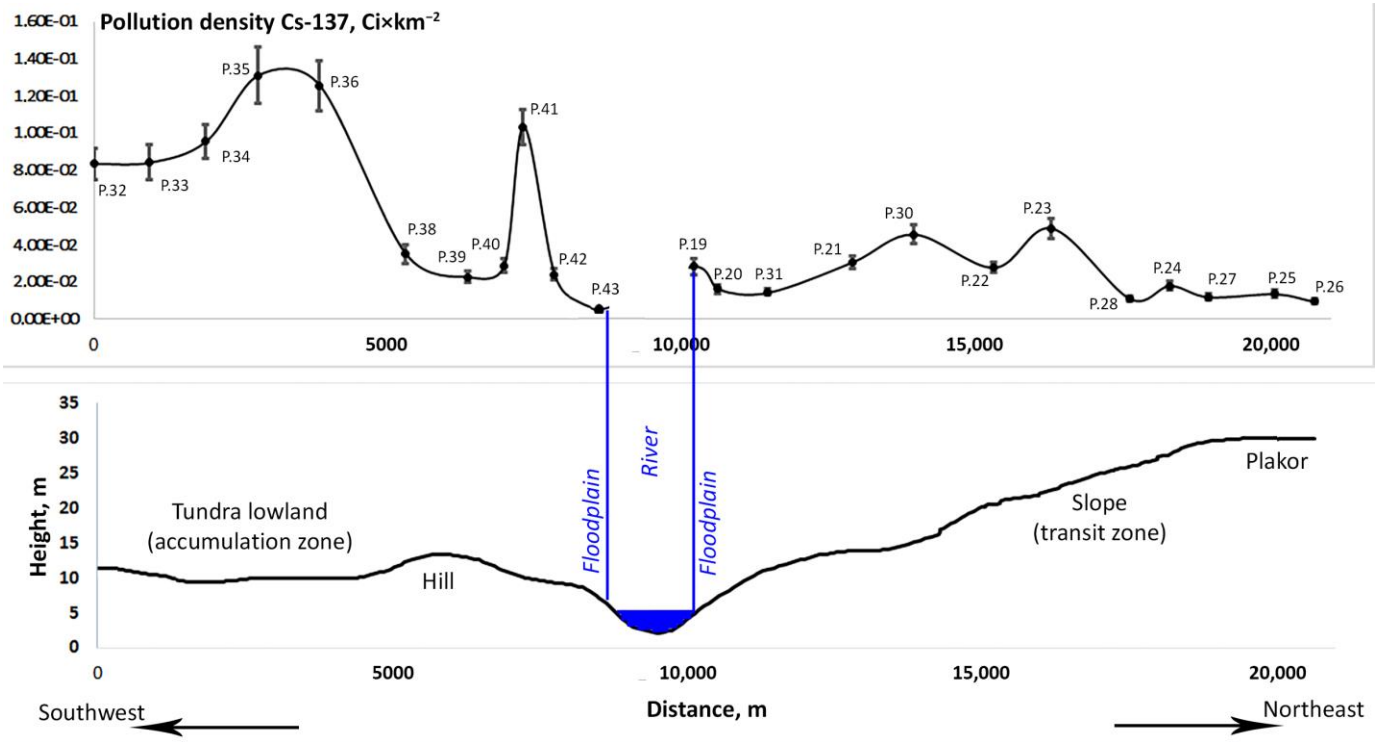

Figure 3. Cs-137 pollution density.

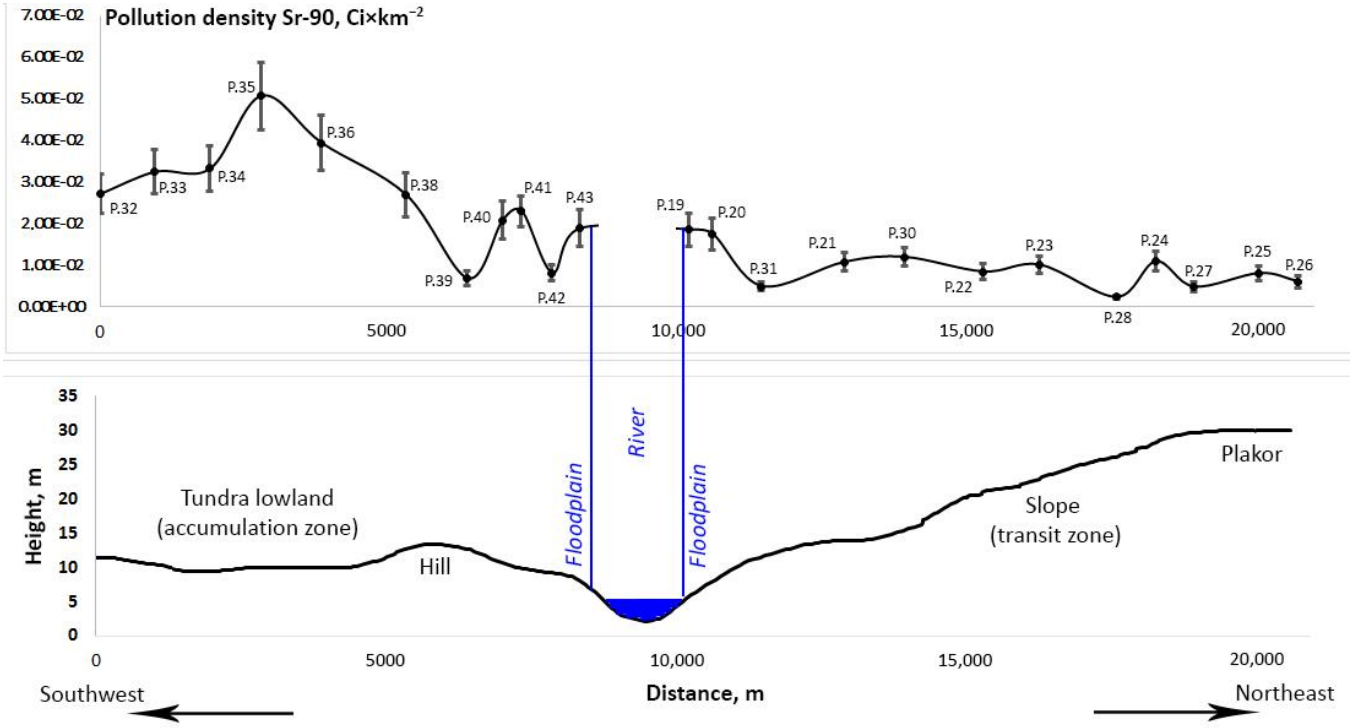

Figure 4. Sr-90 pollution density.

Cs-137 pollution density ranges from 9.22×10^{-3} (3.41×10^{2}) Ci·km^{-2} (Bq×m^{-2}) to 1.31×10^{-1} (4.85×10^{3}) Ci×km^{-2} (Bq×m^{-2}) with a mean of 4.43×10^{-2} (1.64×10^{3}) Ci×km^{-2} (Bq×m^{-2}). Sr-90 pollution density ranges from 2.29×10^{-3} (8.26×10^{1}) Ci×km^{-2} (Bq×m^{-2}) to 5.07×10^{-2} (1.88×10^{3}) Ci×km^{-2} (Bq×m^{-2}) with a mean of 1.74×10^{-2} (6.44×10^{2}) Ci×km$^{-2\,(Bq \times m^{-2})}$. The distribution patterns of Cs-137 and Sr-90 activity in the samples are similar in many respects (Figures 3 and 4). However, marked differences can be seen between the density of Cs-137 and Sr-90 pollution on the slope, in the plakor zone, and within the tundra lowlands. The highest density of Cs-137 and Sr-90 contamination was found in the tundra lowland zone. We assume that anthropogenic radionuclides in this zone are mainly subject to downward migration. The zones of the plakor, slope, and hilly part of the profile are characterized by decreased pollution density, which is caused by more intensive lateral migration and planar washout (surface runoff).

When comparing these findings with previous scarce data on Cs-137 activity levels in the Nenets Autonomous Okrug, a decrease in radiocaesium activity can be observed. According to [43], in the period from 1994 to 2000, Cs-137 levels up to 2000 Bq×kg^{-1} were observed in some samples from the southern part of the Kanin Peninsula. The author accounted this abnormality to nuclear testing carried out in the Novaya Zemlya archipelago; however, they failed to substantiate this claim. Table S1 of this study illustrates that Cs-137 activity within the peat can reach 191.5 ± 17.2 Bq×kg^{-1}.

Due to methodological (instrumental) difficulties, information on Sr-90 pollution densities in general on the territory of the Russian Federation is not known. Consequently, the recently obtained data on Sr-90 content in peats from the western region of the Nenets Autonomous Okrug are new and allow us to estimate the stock of this radionuclide in the tundra area. When comparing Sr-90 results in the Kanin tundra to data obtained in other Arctic regions of Russia and worldwide, an excess of two to three times is evident. Peat profiles in the southern region of Svalbard, for instance, exhibit Sr-90 activity of up to 17.36 Bq×kg^{-1} ± 0.70 Bq×kg^{-1} [44]. In the peat bogs of Northwest Russia's Murmansk region, Sr-90 activity remains within the range of 7.7 Bq×kg^{-1} ± 3.4 Bq×kg^{-1}, as stated by [45]. Table S1 of this study illustrates that Sr-90 activity within the peat can reach 42.8 ± 10.0 Bq×kg^{-1}.

The initial studies of anthropogenic radioactivity on the territory of the Nenets Autonomous Okrug were carried out in 1990–1992 in the form of a radiometric airborne gamma survey to identify ecologically unfavorable areas [46]. Several small areas were found to have a clear anthropogenic impact, with pollution levels surpassing 0.15 Ci×km^{-2} (as of 1992). However, the Nes River basin does not appear to be an area of elevated Cs-137 content, with a pollution density of around 0.1 Ci×km^{-2} (Figure 5). The variation between the outcomes from the current field studies and those of the airborne gamma survey can be explained by the instrumental peculiarities of the airborne gamma survey and the considerable waterlogging of the area, which makes it difficult to register gamma radiation from Cs-137 [47–49].

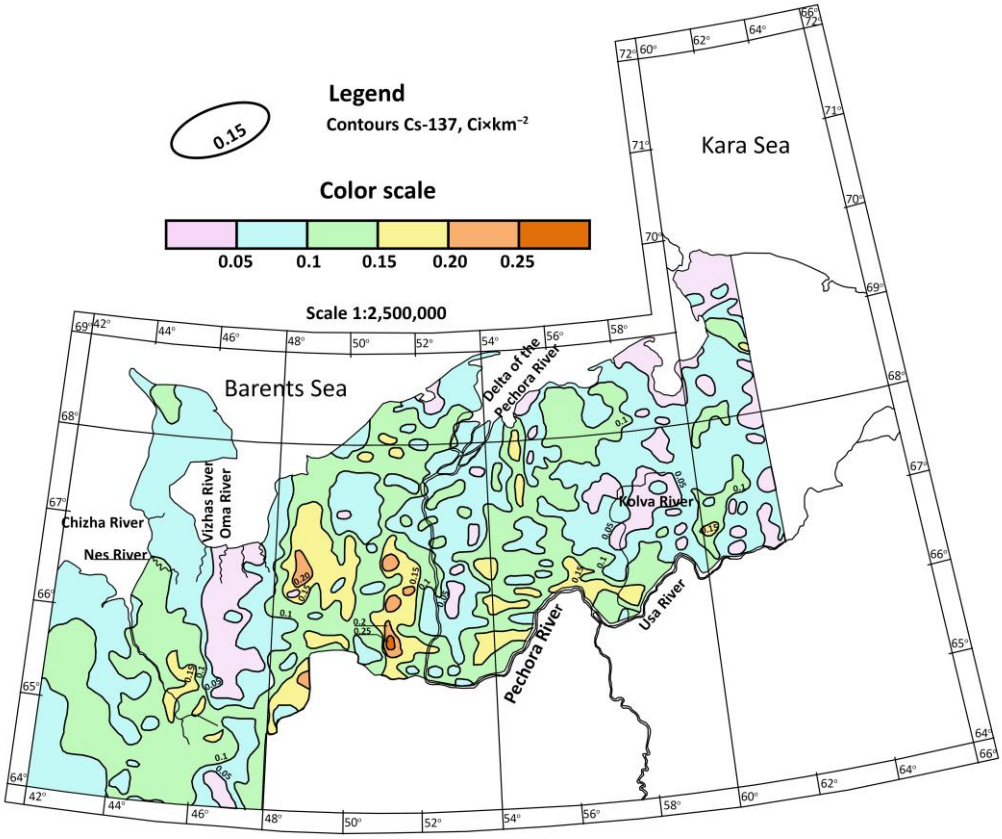

Figure 5. Map of Cs-137 distribution in soils on the territory of the Nenets Autonomous Okrug (Northwest Russia, airborne gamma survey method, results refer to 1992) [46].

Figure 6 shows the spatial distribution plots of the pollution density of Am-241, Pu-238, and Pu-239+240. The nature of their distribution is not clear but is generally similar to that of Cs-137 and Sr-90.

The pollution density of Am-241 ranges from 8.69 × 10^{-5} (3.22) Ci×km^{-2} (Bq×m^{-2}) to 1.11 × 10^{-3} (41.1) Ci×km^{-2} (Bq×m^{-2}), with an average of 4.36 × 10^{-4} (16.1) Ci×km^{-2} (Bq×m^{-2}). The pollution density of Pu-238 ranges from 1.84 × 10^{-5} (0.68) Ci×km^{-2} (Bq×m^{-2}) to 3.17 × 10^{-4} (11.7) Ci×km^{-2} (Bq×m^{-2}), with an average of 1.10 × 10^{-4} (4.07) Ci×km^{-2} (Bq×m^{-2}). The pollution density of Pu-239+240 ranges from 8.18 × 10^{-5} (3.03) Ci×km^{-2} (Bq×m^{-2}) to 4.04 × 10^{-3} (150.0) Ci×km^{-2} (Bq×m^{-2}), with an average of 1.08 × 10^{-3} (40.0) Ci×km^{-2} (Bq×m^{-2}). In several locations, these radionuclides were not detected as their measured values were below the MDA.

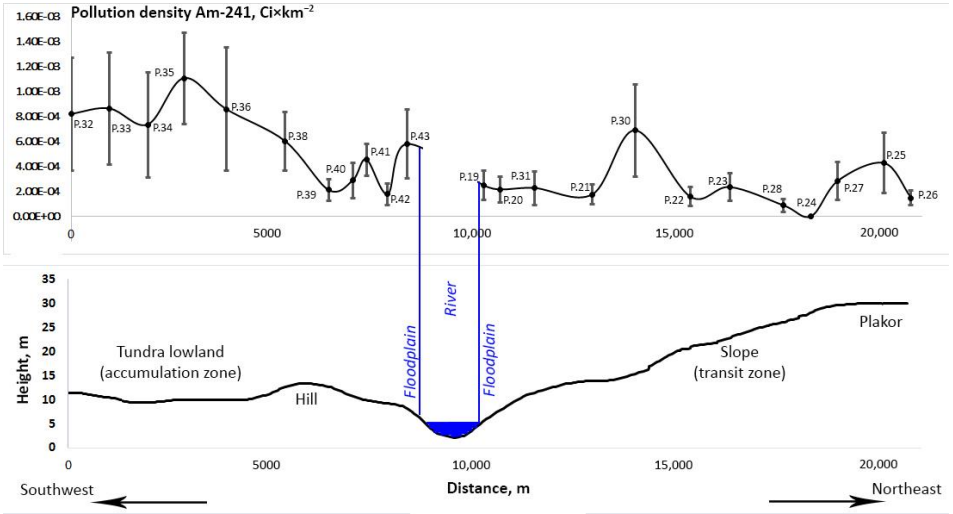

(**a**)

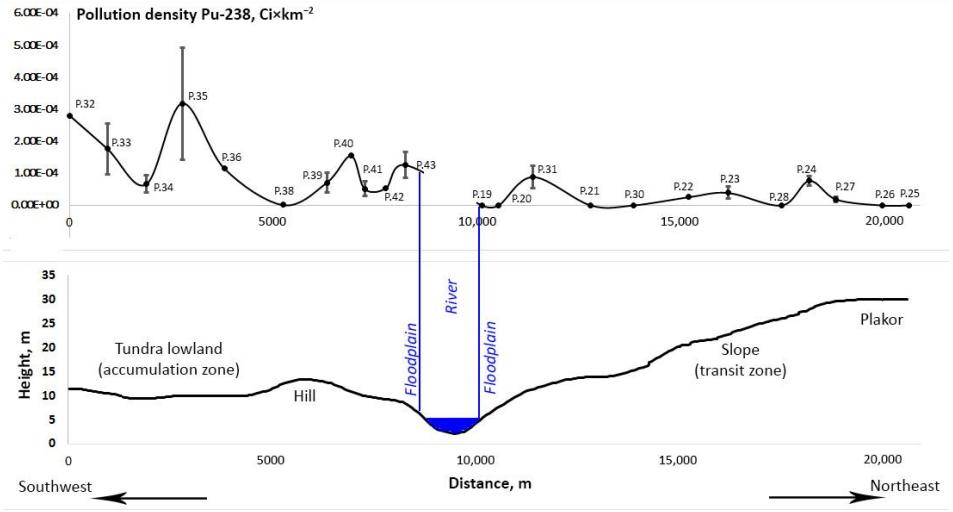

(**b**)

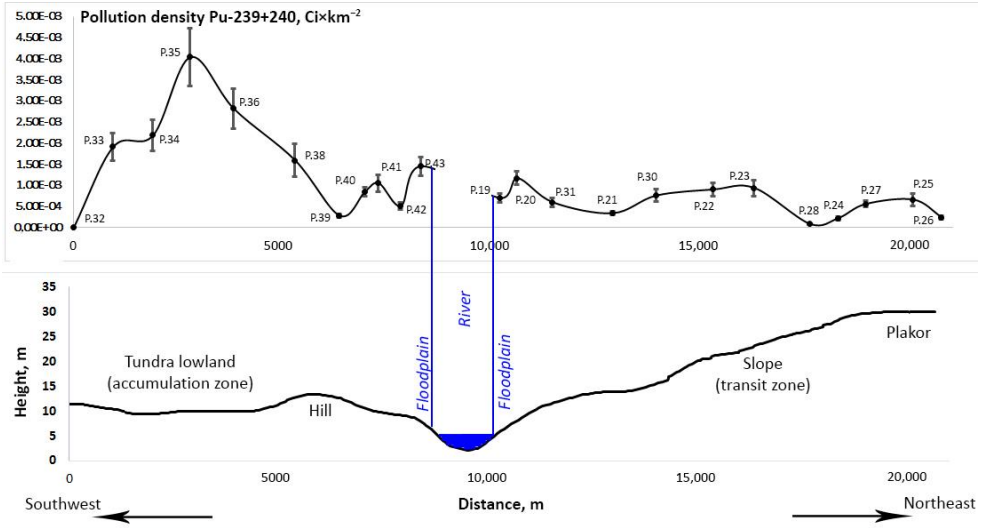

(**c**)

Figure 6. Am-241 (**a**), Pu-238 (**b**), Pu-239+240, (**c**) pollution density.

As with Sr-90, Am-241, Pu-238, and Pu-239+240 have not been the subject of indepth research in the Nenets Autonomous Okrug. The estimated content of these radionuclides is found in the Mezenskiy and Primorskiy districts of the Arkhangelsk region. Thus, based on [24], the activities of Pu-239 and Pu-240 in organogenic soils within the Arkhangelsk region predominantly fall within the range of minimum measured activities up to 4 $Bq \times kg^{-1}$. In [24], the plutonium isotope content was determined by mass spectrometry, so Pu-239 and Pu-240 were measured separately. The activity of Am-241 does not surpass 3 $Bq \times kg^{-1}$. Comparable levels of these radionuclides can be observed in more northern regions, such as Svalbard, where Am-241 activity generally does not exceed 3–4 $Bq \times kg^{-1}$ but can reach up to 11 $Bq \times kg^{-1}$ in certain peat layers [23]. The activity of Pu-239+240 in Svalbard is predominantly within the range of up to 5–6 $Bq \times kg^{-1}$, with sporadic occurrences in certain layers where it reaches 23 $Bq \times kg^{-1}$. According to the results of isotopic ratios in [24] and [23], the main sources of radionuclide pollution are global atmospheric fallout and the Chernobyl accident. Yakovlev [24] also identifies tests carried out on the Novaya Zemlya archipelago as an additional source of pollution. The levels of plutonium and americium isotopes found in peat on the Kanin tundra are similar to those recorded in the Arkhangelsk region and on Spitsbergen Island (see Table S1). The activity of Am-241 in the Nes River basin territory does not surpass 1.4 ± 0.7 $Bq \times kg^{-1}$, Pu-238—0.41 ± 0.12 $Bq \times kg^{-1}$, Pu-239+240—3.4 ± 0.6 $Bq \times kg^{-1}$.

3.2. Vertical Distribution of Anthropogenic Radionuclides

Figures 7 and 8 present the calculated isotopic ratios of $Cs\text{-}137_{horizon\ 10–20\ cm}/Cs\text{-}137_{horizon\ 0–10\ cm}$ and $Sr\text{-}90_{horizon\ 10–20\ cm}/Sr\text{-}90_{horizon\ 0–10\ cm}$.

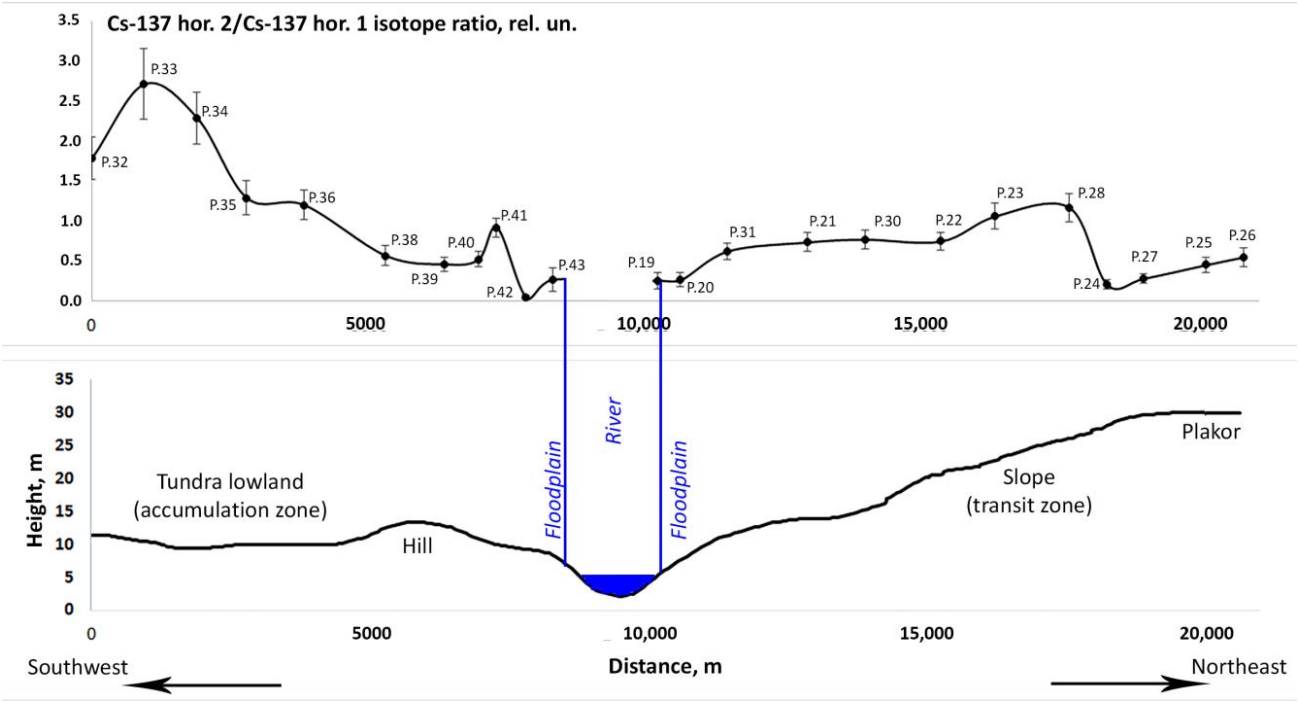

Figure 7. Features of Cs-137 migration based on isotope ratio.

In the lowland tundra zone located southwest of the Nes River basin, there is a marked vertical migration of Cs-137 observed along the 0–20 cm profile with an isotopic ratio greater than 1 for the two layers. In certain lowland areas, the activity of Cs-137 in the 10–20 cm layer surpasses the activity in the 0–10 cm layer by more than twice. A comparable pattern of migration was reported by [50] for a peat section in the Salym area of lowland Khanty-Mansiysk Autonomous Okrug in Russia. Higher Cs-137 activities are observed at a depth of 10–15 cm compared to the overlying layers.

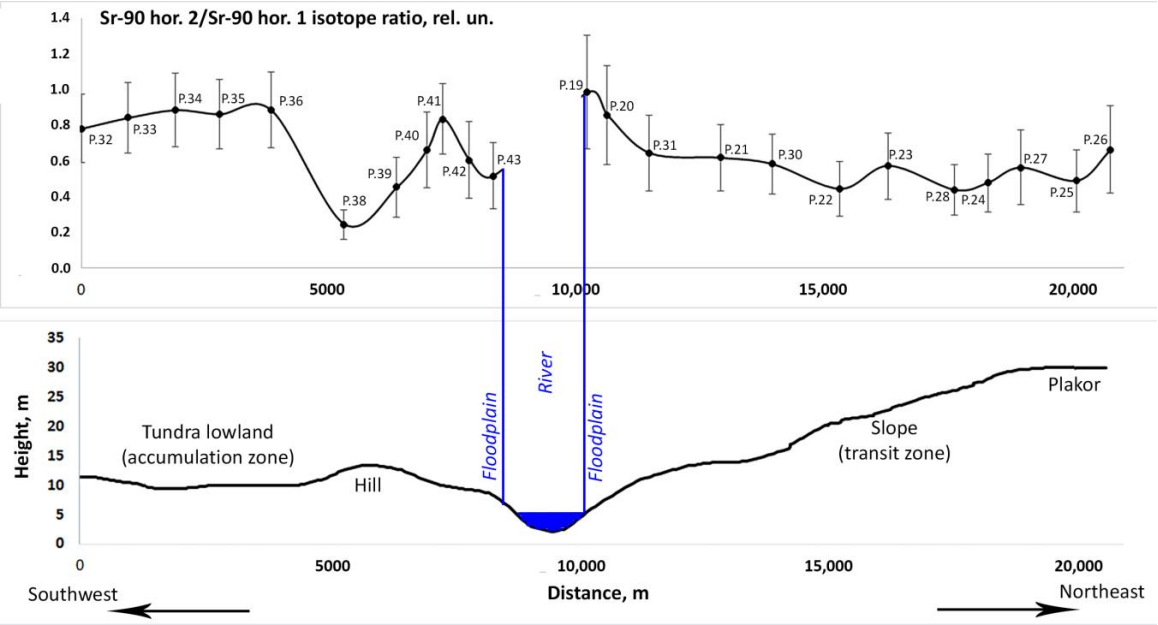

Figure 8. Features of Sr-90 migration based on isotope ratio.

A low level of vertical migration of radionuclides (isotope ratio for two layers < 1) is observed in the hill, slope, and plakor zones. This may be due to a more intensive runoff process along the sampling profile, resulting in an increase in radionuclide activity towards the lower part of the slope. Similarly, the distribution of Sr-90 in the areas of tundra lowland and slope bears resemblance to the radionuclide Cs-137. A stronger vertical migration trend is observed for Cs-137 compared to Sr-90. Several other studies [51] have demonstrated a similar migration pattern of anthropogenic radionuclides through variations in relief structure.

Although Sr-90 has higher mobility in soils, this study's results indicate that its behavior and that of Cs-137 are quite similar in many ways. This may be due to the fact that postsedimentation mobility of radionuclides in soils decreases in arctic conditions, which are characterized by long periods of low temperatures, slow decomposition of organic matter, and minimal bioturbation [23]. Permafrost is a crucial factor hindering deep water infiltration in peat deposits and often results in waterlogging of the active peat layer, which is situated above mineral soils and is seasonally thawed. According to [52], the Nes River basin is situated in the cryolithozone with a discontinuous distribution of permafrost. The seasonally thawed layer's average depth up to 20 km from the Nes River mouth is 0.4 m.

No peculiarities of Am-241, Pu-238, and Pu-239+240 distribution in two layers in different landforms are observed (Figure 9). Most likely, it is connected to the low content of these radionuclides in samples.

The impact of relief on the migration of elements, including radionuclides, has been studied for a long time. For instance, Klimova [53] observed a substantial build-up of Cs-137 in lowland areas, while hilly areas are characterized by the transit character of the lateral migration of the radionuclide. Additionally, the study highlights the intensified migration of radionuclides in the presence of high soil moisture and water stagnation in depressions. These phenomena are observable in the tundra lowland area southwest of Nes's village. Radionuclides Cs-137 and Sr-90 have significantly accumulated here, and their migration along the vertical profile is the most prevalent. The examination of increased activity in upper soil layers down the slope was also investigated in [54]. The incline with a gradient of 10 degrees resulted in a rise in Cs-137 and Am-241 radionuclide activity levels by 54% and 29%, respectively. In landscape–geochemical systems of the "plakor–slope–lowland" kind, cyclic variation of radionuclide markers Cs-137 and Sr-90 in soils was identified based on research [55]. The variability structure of both markers was similar but not identical, attributed to the differing chemical properties and migration peculiarities of these radionuclides. Earlier,

it was noted that the Nes River basin exhibits similar migration properties for Cs-137 and Sr-90 radionuclides, although a more intensive migration is observed for Cs-137.

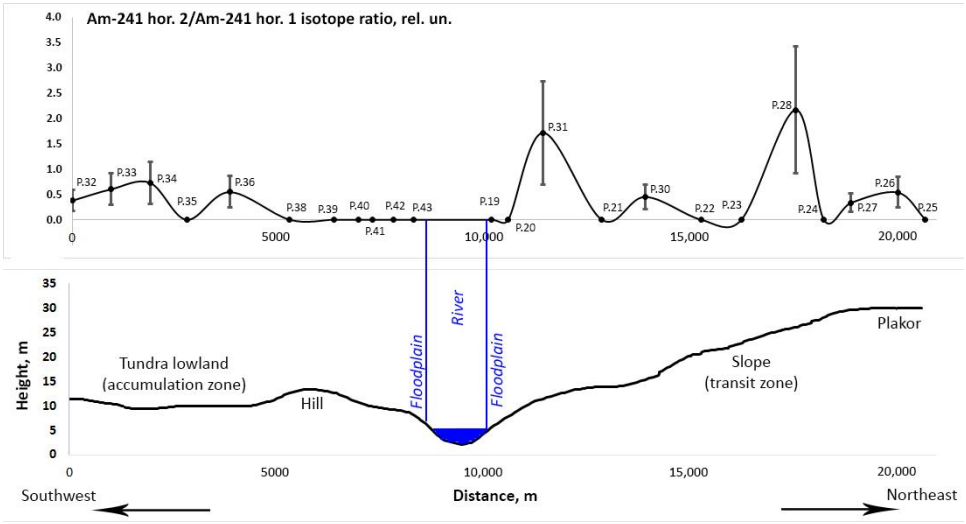

(**a**)

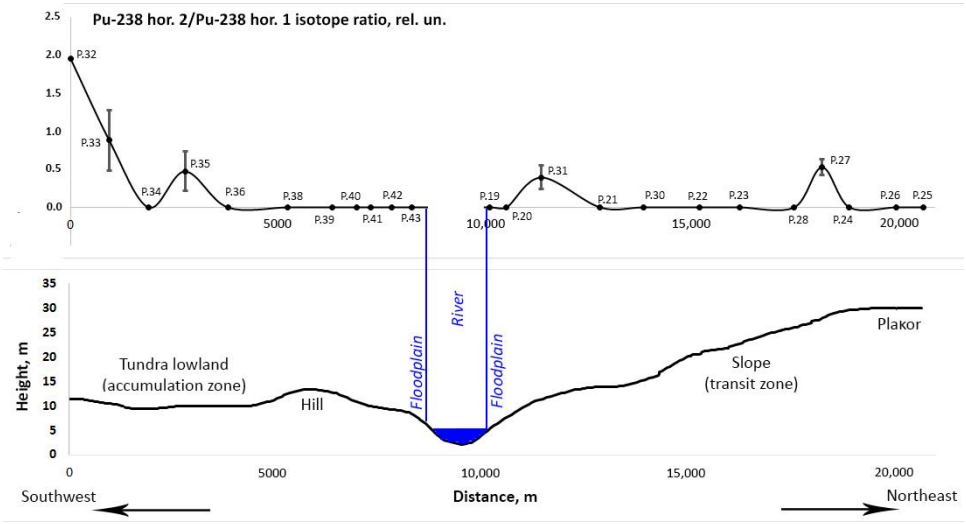

(**b**)

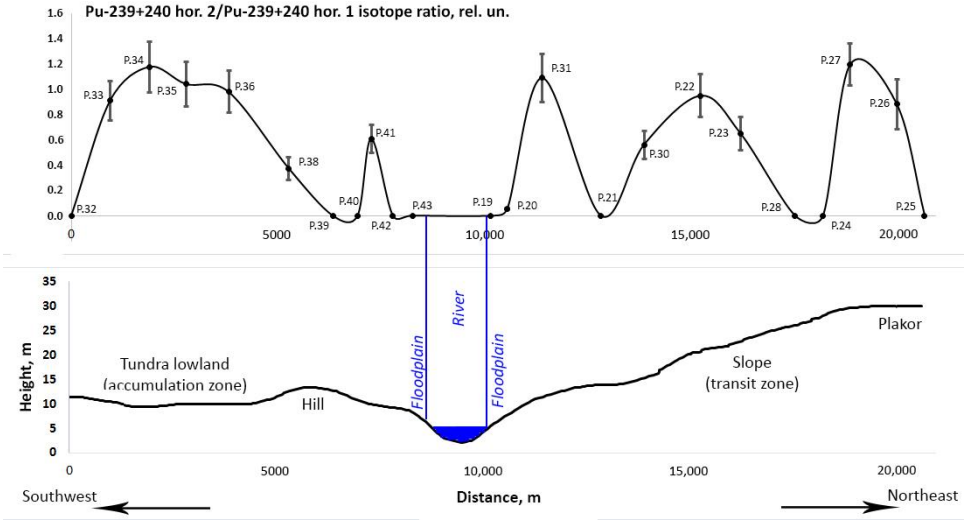

(**c**)

Figure 9. Features of Am-241 (**a**), Pu-238 (**b**), and Pu-239+240 (**c**) migration based on isotope ratio.

It is evident that in assessing the flushing of radionuclides by surface runoff in undisturbed peat areas, it is crucial to be aware of the radionuclide concentration in the upper few millimeters of peat [55]. Furthermore, in order to identify the characteristics of vertical migration, it is essential to extract soil and peat cores from a depth of at least 50 cm owing to the varying degree of deep migration of anthropogenic radionuclides [24]. However, using radionuclide activity ratios in various layers (specifically 0–10 cm and 10–20 cm), this study has distinguished differences in radionuclide activity across important relief structures (plakor, slope, and lowland areas). The obtained outcomes are consistent with prior research, yet they also provide new insights into inadequately researched regions, such as the tundra areas in the subarctic zone of Russia.

3.3. Estimation of Pollution Sources Based on Isotope Ratio Calculations and HYSPLIT Air Mass Trajectory Model

To determine probable sources of radionuclide pollution, we performed calculations for isotopic ratios of Sr-90/Cs-137, Pu-238/Pu-239+240, Pu-239+240/Cs-137, and Am-241/Pu-239+240, and created linear regression plots depicting the correlations between these radionuclides (Figure 10).

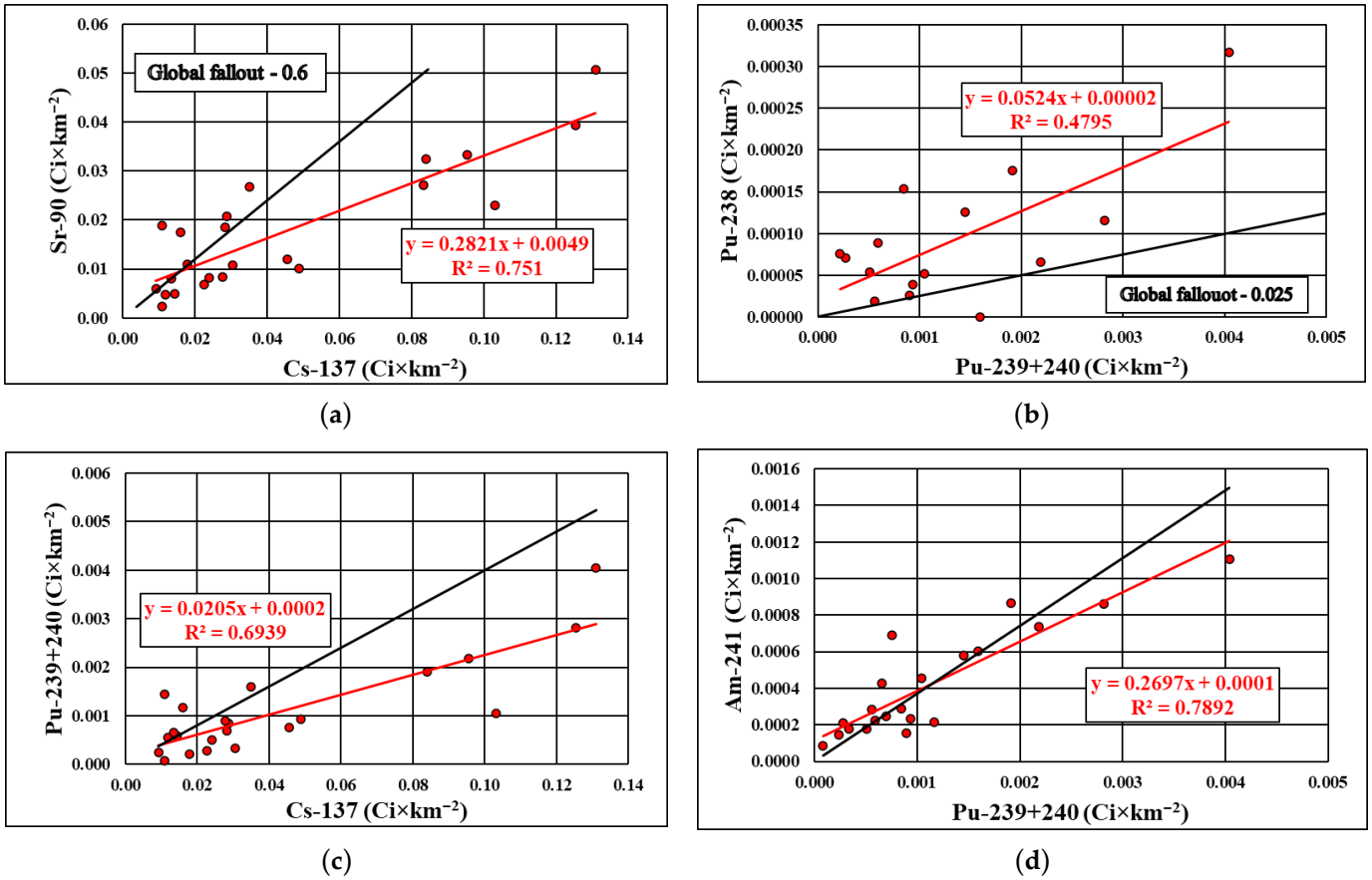

Figure 10. Linear regression plots to assess the relationships between (**a**) Cs-137 and Sr-90, (**b**) Pu-238 and Pu-239+240, (**c**) Pu-239+240 and Cs-137, and (**d**) Am-241 and Pu-239+240.

The R^2 values presented in Figure 10 are not relevant to this study. Table 1 illustrates the computed mean isotope ratio and slope of the linear regression model for the Nes River basin, together with a comparison to data gathered from Svalbard Island [29].

Table 1. Results of calculation of isotopic ratios of anthropogenic radionuclides in peat of the Nes River basin.

Radionuclide	Isotopic Ratio, rel. un.				
	Nes River Basin		Svalbard Island		Global Fallout
	Average Value	Regression Slope	Average Value	Regression Slope	
Sr-90/ Cs-137	0.501	0.2821	-	-	0.6 *
Pu-238/ Pu-239+240	0.102	0.0524	0.034	0.0231	0.025 **
Pu-239+240/ Cs-137	0.0323	0.0205	0.06	0.0622	0.04 **
Am-241/ Pu-239+240	0.46	0.2697	0.46	0.4161	0.37 **

Notes: * According to [56]. ** According to [25].

Isotope ratio calculations reveal that none of the results obtained for the Kanin tundra match the characteristics of global fallout. The average values of Sr-90/Cs-137 and Am-241/Pu-239+240 ratios are similar to those of global fallout. However, because the regression slope significantly deviates from the mean value, it suggests that these results do not reflect a single source of pollution. Furthermore, the isotopic ratio of Am-241/Pu-239+240 in global fallout is continually rising as a result of the growing Am-241 activity owing to the decay of Pu-241. This hinders the usage of this parameter in evaluating the origin of pollution. It is worth mentioning the resemblance of the findings, both in terms of the average value parameter and regression slope, to those of Lokas et al. [23,27–29]. Based on the studies conducted, it can be inferred that the primary contributors to radionuclide pollution on Svalbard are the global atmospheric fallout and the Chernobyl accident. As a result, it is reasonable to assume that the same sources, as well as possible local tropospheric fallout from nuclear tests on the Novaya Zemlya archipelago, are responsible for the pollution observed in the Nes River basin. The presence of the Chernobyl fallout is verified through the Pu-238/Pu-239+240 isotopic ratio mean values (0.102) and regression slope (0.0524) in the study area, which differ marginally from the global fallout's value (0.025). According to [26,30,57], excessive Pu-238 content characterizes the Chernobyl fallout, and the Pu-238/Pu-239+240 isotopic ratio ranges from 0.19 to 0.55. This explains the excess Pu-238 content in the study area.

Additional data for analyzing sources of radioactive pollution is obtained by calculating pollution trajectories using the widely used HYSPLIT model [58]. The methodology involves acquiring a set of air mass trajectories from specific sources based on meteorological parameters [58]. The chosen sources were thermonuclear explosions and nuclear fission-based tests executed on the Novaya Zemlya archipelago between 1955 and 1962 [59]. Due to the significant number of tests (132 tests, of which 87 were airborne), the largest explosions (at least 10 kilotons yield for fission tests and at least 100 kilotons yield for thermonuclear explosions) were used to calculate the trajectories. A total of 46 nuclear tests were taken into account. The results of the trajectory calculations showed that the air masses following these explosions moved north, west, and east. Western transportation frequently resulted in atmospheric fallout on the continent, such as on the Yamal Peninsula in Russia. Figure 11a–d illustrates air mass trajectories along the primary directions. The nearest trajectory to the research area is associated with the airborne nuclear test at the Sukhoi Nos site on 02.10.1958 with a power of 40 kilotons (Figure 11d). Trajectories are shown at three altitudes—500, 1000 and 1500 m. No additional trajectories were found towards the Kanin Peninsula, encompassing the Nes River basin territory. This suggests that local (tropospheric) fallout is unlikely to be the source of pollution in the Nes River basin.

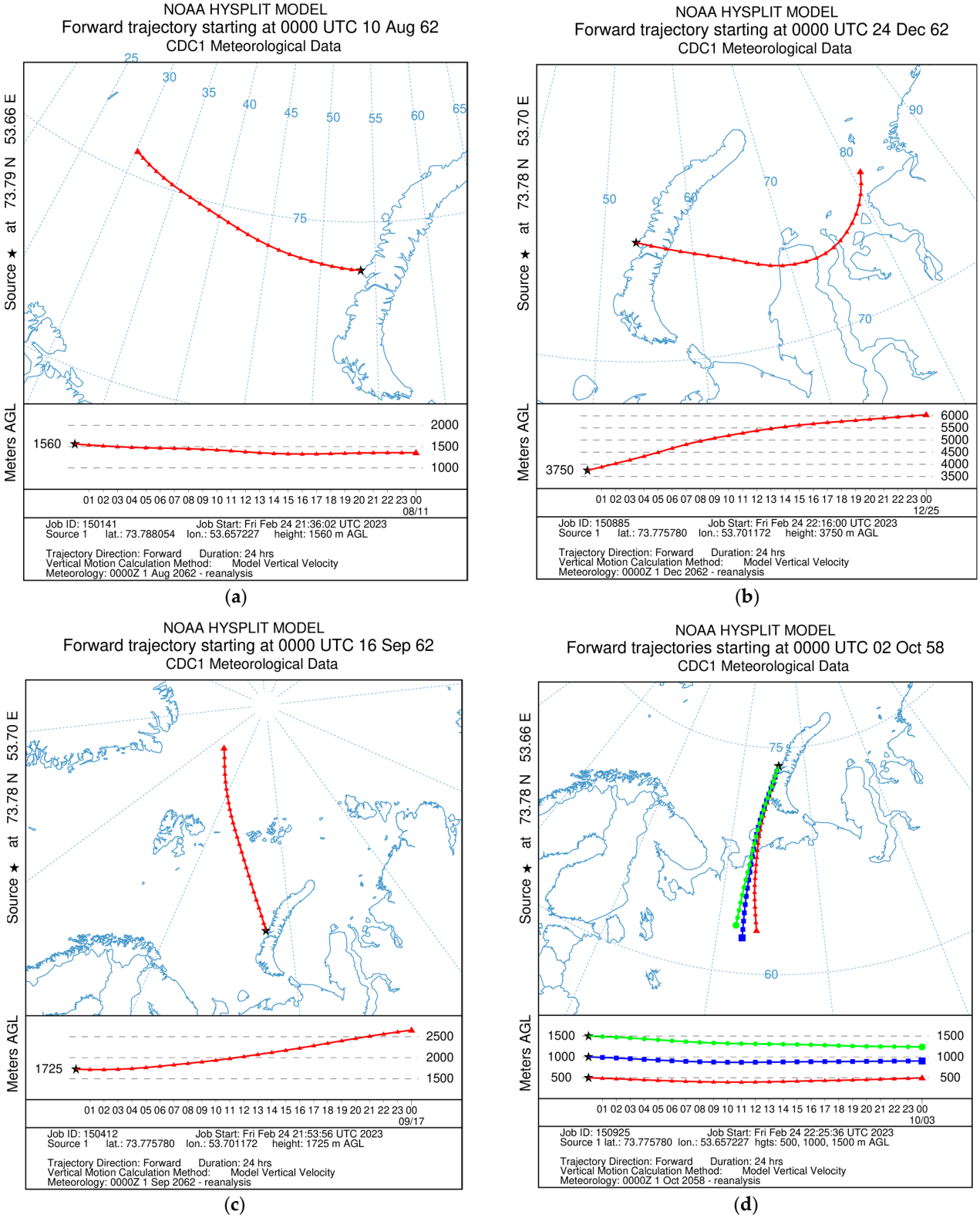

Figure 11. Main trajectories of air masses (HYSPLIT model). (**a**) atmospheric nuclear test at the site Sukhoi Nos, D-2, at an altitude of 1560 m, power—400 kt, 10 August 1962; (**b**) atmospheric thermonuclear test at the site Sukhoi Nos, D-2, at an altitude of 3750 m, power—24,200 kt, 24 December 1962; (**c**) atmospheric thermonuclear test at the site Sukhoi Nos, D-2, height unknown, power—3250 kt, 16 September 1962; (**d**) atmospheric nuclear test at the site Sukhoi Nos, D-2, height unknown, power—40 kt, 2 October 1958 [38].

4. Conclusions

This paper assesses the content of anthropogenic radionuclides in tundra landscapes of the subarctic zone of Russia in the Nenets Autonomous Okrug. It examines the accumulation and migration patterns of these radionuclides. The study identifies possible sources of environmental pollution by calculating the isotopic ratios of Sr-90/Cs-137, Pu-238/Pu-239+240, Pu-239+240/Cs-137, and Am-241/Pu-239+240, and by determining pollution trajectories using the HYSPLIT model. The study's findings revealed that the Nes River basin has a radionuclide Cs-137 and Sr-90 pollution density that is two to three times higher than its available data for the Kaninskaya tundra, as well as for Russia and the world in general. This confirms the existence of a region with an increased content of radionuclides. The isotope ratio calculations conducted for layers at depths of 10–20 cm and 0–10 cm indicate that some parts of the tundra, specifically the tundra lowlands, exhibit signs of technogenic radionuclide accumulation and subsequent vertical migration. Conversely, the slopes, plakor, and hilly regions have a greater level of lateral migration, leading to reduced anthropogenic radionuclide activity in peat. Calculation of isotopic ratios of anthropogenic radionuclides and the air mass trajectory using the HYSPLIT model have indicated that the primary sources of pollution pertaining to anthropogenic radionuclides are the global atmospheric fallout and the Chernobyl accident.

Supplementary Materials: The following supporting information can be downloaded at https://www.mdpi.com/article/10.3390/app132312952/s1, Table S1: Activity and pollution density of anthropogenic radionuclides in the Nes River basin (Nenets Autonomous Okrug).

Author Contributions: A.P.: Conceptualization, Investigation, Methodology, Validation, Resources, Supervision, Project administration, Funding acquisition, Writing. E.Y.: Conceptualization, Investigation, Methodology, Validation, Formal analysis, Writing, Review & Editing. All authors have read and agreed to the published version of the manuscript.

Funding: This research was funded by a grant from the Russian Science Foundation, number 22-27-20079.

Institutional Review Board Statement: Not applicable.

Informed Consent Statement: Not applicable.

Data Availability Statement: Data is contained in the Supplementary Materials.

Conflicts of Interest: The authors declare that they have no known competing financial interests or personal relationships that could have appeared to influence the work reported in this paper.

References

1. Ahmed, A.; Qian, X.; Peng, B.X.T.; Chen, Z.; Choudhary, A.; Hussain, A. Floaters for Oil and Gas Exploration in the Arctic—A Review. In Proceedings of the Offshore Technology Conference Asia, Kuala Lumpur, Malaysia, 22–25 March 2016.
2. Bergmann, M.; Collard, F.; Fabres, J.; Gabrielsen, G.W.; Provencher, J.F.; Rochman, C.M.; van Sebille, E.; Tekman, M.B. Plastic pollution in the Arctic. *Nat. Rev. Earth Environ.* **2022**, *3*, 323–337. [CrossRef]
3. Brodt, L.E. Best Practices of Oil and Gas Companies to Develop Gas Fields on the Arctic Shelf. *Arct. North* **2021**, *44*, 30–44. [CrossRef]
4. Latva, O.; Tynkkynen, N. The Problem of Plastic in the Arctic. In *Cold Waters. Tangible and Symbolic Seascapes of the North*; Lehtimäki, M., Rosenholm, A., Trubina, E., Tynkkynen, N., Eds.; Springer: Cham, Switzerland, 2022; pp. 3–17. [CrossRef]
5. Madani, N.; Parazoo, N.C.; E Miller, C. Climate change is enforcing physiological changes in Arctic Ecosystems. *Environ. Res. Lett.* **2023**, *18*, 074027. [CrossRef]
6. Pelaudeix, C. *Governance of Arctic Offshore Oil and Gas*; Routledge: London, UK, 2017.
7. Schmale, J.; Arnold, S.R.; Law, K.S.; Thorp, T.; Anenberg, S.; Simpson, W.R.; Mao, J.; Pratt, K.A. Local Arctic Air Pollution: A Neglected but Serious Problem. *Earth's Future* **2018**, *6*, 1385–1412. [CrossRef]
8. Sorokina, T.; Trubina, A.; Tynkkynen, E. Pollution and Monitoring in the Arctic. In *Cold Waters. Tangible and Symbolic Seascapes of the North*; Lehtimäki, M., Rosenholm, N., Eds.; Springer: Cham, Switzerland, 2022; pp. 229–253. [CrossRef]
9. Tudorache, V.-P.; Antonescu, N.-N. Challenges of oil and gas exploration in the Arctic. *J. Eng. Sci. Innov.* **2020**, *5*, 273–286. [CrossRef]
10. Wangberg, S.A.; Bjork, G. Pollution in the Arctic Ocean. In *Anthropogenic Pollution of Aquatic Ecosystems*; Häder, D.-P., Helbling, E.W., Villafane, V.E., Eds.; Springer Nature: Berlin, Germany, 2021; pp. 91–111. [CrossRef]

11. Epifanova, I.E.; Epifanov, A.O. On the issue of control of the Barents sea radioecological situation's. *Int. J. Appl. Fundam. Res.* **2020**, *10*, 16–21.
12. Livingston, H.D.; Povinec, P.P. A millennium perspective on the contribution of global fallout radionuclides to ocean science. *Heal. Phys.* **2002**, *82*, 656–668. [CrossRef]
13. Matishov, G.G.; Ilyin, G.V.; Usyagina, I.S.; Kirillova, E.E. Dynamics of artificial radionuclides in the ecosystems of seas of the arctic ocean at the turn of the 21st century. Part 2. Bottom sediments. *Sci. South Russ.* **2019**, *15*, 24–35. [CrossRef]
14. Matishov, G.G.; Kasatkina, N.E.; Usyagina, I.S. Technogenic Radioactivity of Waters in the Central Arctic Basin and Adjacent Water Areas. *Dokl. Earth Sci.* **2019**, *485*, 288–292. [CrossRef]
15. *AMAP Assessment 2015: Radioactivity in the Arctic*; Arctic Monitoring and Assessment Programme (AMAP): Oslo, Norway, 2015.
16. Chen, J.; Zhang, W.; Sadi, B.; Wang, X.; Muir, D.C. Activity concentration measurements of selected radionuclides in seals from Canadian Arctic. *J. Environ. Radioact.* **2017**, *169–170*, 48–55. [CrossRef]
17. Cwanek, A.; Mietelski, J.W.; Łokas, E.; Olech, M.A.; Anczkiewicz, R.; Misiak, R. Sources and variation of isotopic ratio of airborne radionuclides in Western Arctic lichens and mosses. *Chemosphere* **2019**, *239*, 124783. [CrossRef] [PubMed]
18. Friedlander, B.R.; Gochfeld, M.; Burger, J. Radionuclides in the marine environment: A CRESP science review. In *Amchitka Independent Science Assessment: Biological and Geophysical Aspects of Potential Radionuclide Exposure in the Amchitka Marine Environment*; Consortium for Risk Evaluation with Stakeholder Participation; Powers, C.W., Burger, J., Kosson, D., Gochfeld, M., Barnes, D., Eds.; IEEE Access: Piscataway, NJ, USA, 2005; pp. 1–95.
19. Miroshnikov, A.Y.; Laverov, N.P.; Chernov, R.A.; Kudikov, A.V.; Ysacheva, A.A.; Semenkov, I.N.; Aliev, R.A.; Asadulin, E.E.; Gavrilo, M.V. Radioecological investigations on the Northern Novaya Zemlya Archipelago. *Oceanology* **2017**, *57*, 204–214. [CrossRef]
20. Nielsen, S.P.; Lüning, M.; Ilus, E.; Outola, I.; Ikaheimonen, T.; Mattila, J.; Herrman, J.; Kanisch, G.; Osvath, I. Baltic Sea: Radionuclides. In *Radionuclides in the Environment*, 2nd ed.; Atwood, D.A., Ed.; Wiley: New York, NY, USA, 2010; pp. 1–22. [CrossRef]
21. Saniewski, M.; Wietrzyk-Pełka, P.; Zalewska, T.; Olech, M.; Węgrzyn, M.H. Bryophytes and lichens as fallout originated radionuclide indicators in the Svalbard archipelago (High Arctic). *Polar Sci.* **2020**, *25*, 100536. [CrossRef]
22. ACIA (Arctic Climate Impact Assessment). *Impacts of a Warming Arctic: Arctic Climate Impact Assessment*; Cambridge University Press: Cambridge, UK; New York, NY, USA, 2004; p. 144.
23. Łokas, E.; Mietelski, J.; Ketterer, M.; Kleszcz, K.; Wachniew, P.; Michalska, S.; Miecznik, M. Sources and vertical distribution of 137Cs, 238Pu, 239+240Pu and 241Am in peat profiles from southwest Spitsbergen. *Appl. Geochem.* **2013**, *28*, 100–108. [CrossRef]
24. Yakovlev, E.; Spirov, R.; Druzhinin, S.; Ocheretenko, A.; Druzhinina, A.; Mishchenko, E.; Zhukovskaya, E. Atmospheric fallout of radionuclides in peat bogs in the Western Segment of the Russian Arctic. *Environ. Sci. Pollut. Res.* **2021**, *28*, 25460–25478. [CrossRef] [PubMed]
25. Holm, E.; Rioseco, J.; Pettersson, H. Fallout of transuranium elements following the Chernobyl accident. *J. Radioanal. Nucl. Chem.* **1992**, *156*, 183–200. [CrossRef]
26. Kershaw, P.; Baxter, A. The transfer of reprocessing wastes from north-west Europe to the Arctic. *Deep Sea Res. Part II Top. Stud. Oceanogr.* **1995**, *42*, 1413–1448. [CrossRef]
27. Łokas, E.; Anczkiewicz, R.; Kierepko, R.; Mietelski, J. Variations in Pu isotopic composition in soils from the Spitsbergen (Norway): Three potential pollution sources of the Arctic region. *Chemosphere* **2017**, *178*, 231–238. [CrossRef]
28. Łokas, E.; Wachniew, P.; Baccolo, G.; Gaca, P.; Janko, K.; Milton, A.; Buda, J.; Komędera, K.; Zawierucha, K. Unveiling the extreme environmental radioactivity of cryoconite from a Norwegian glacier. *Sci. Total Environ.* **2022**, *814*, 152656. [CrossRef]
29. Łokas, E.; Zaborska, A.; Kolicka, M.; Różycki, M.; Zawierucha, K. Accumulation of atmospheric radionuclides and heavy metals in cryoconite holes on an Arctic glacier. *Chemosphere* **2016**, *160*, 162–172. [CrossRef]
30. Mietelski, J.W.; Was, B. Plutonium from Chernobyl in Poland. *Appl. Radiat. Isot.* **1995**, *46*, 1203–1211. [CrossRef]
31. UNSCEAR. Sources and Effects of Ionizing Radiation. In *United Nations Scientific Committee on the Effects of Atomic Radiation*; United Nations Publication: New York, NY, USA, 2008. Available online: https://applied%E2%80%93research.ru/ru/article/view?id=10199 (accessed on 1 September 2023).
32. Biblin, A.M.; Khramtsov, E.V.; Ivanov, S.A.; Sednev, K.A.; Georgieva, A.G. *Radiation-Hygienic Research at the Site of the Peaceful Nuclear Explosion "Horizon-1" on the Territory of the Komi Republic; Collection of Abstracts of the All-Russian Scientific-Practical Conference with International Participation "Radiation Hygiene and Continuing Professional Education: New Challenges and Ways of Development"*; Moscow State University: Moscow, Russia, 2022.
33. Bogoyavlensky, V.I.; Perekalin, S.O.; Boichuk, V.M.; Bogoyavlensky, I.V.; Kargina, T.N. Kumzhinskoye Gas Condensate Field Disaster: Reasons, results and ways of eliminating the consequences. *Arct. Ecol. Econ.* **2017**, *25*, 32–46. [CrossRef]
34. Puchkov, A.V.; Druzhinina, A.S.; Yakovlev, E.Y.; Druzhinin, S.V. Assessing the natural and anthropogenic radionuclide activities in fish from Arctic rivers (Northwestern Russia). *Pollution* **2023**, *9*, 1098–1116. [CrossRef]
35. Puchkov, A.; Druzhinina, A.; Yakovlev, E.; Druzhinin, P. Accumulation of radionuclides in fish from the rivers of the northwestern sector of the Russian Arctic. *Arct. Ecol. Econ.* **2023**, *13*, 127–137. [CrossRef]
36. Puchkov, A.; Yakovlev, E. Features of accumulation and migration of technogenic radionuclides Cs-137 and Sr-90 in the tundra landscapes of the Russian Arctic (evidence from the Nes river basin, Kanin tundra). *Vestn. Geosci.* **2023**, *1*, 42–51. [CrossRef]

37. Puchkov, A.; Yakovlev, E.; Druzinin, S. Radiation parameters of hydrobionts of the background territory of the nenets autonomous okrug. *Success Mod. Nat. Sci.* **2020**, *6*, 118–122. [CrossRef]
38. Fortescue, J.A.C. Element Migration in Landscapes. In *Environmental Geochemistry. Ecological Studies*; Springer: New York, NY, USA, 1980; Volume 35. [CrossRef]
39. Gavrilova, I.P.; Kasimov, N.S. *Workshop on Landscape Geochemistry*; Moscow University: Moscow, Russia, 1989; 72p.
40. Linnik, V. *Landscape Differentiation of Technogenic Radionuclides*; ResearchGate: Berlin, Germany, 2018. (In Russian)
41. Perel'man, A.I.; Levin, V.N. Landscape geochemistry and the problems of genesis, exploration, and ecology of uranium de-posits. *Geol. Ore Depos.* **1999**, *41*, 30–35.
42. Tokar', E.; Kuzmenkova, N.; Rozhkova, A.; Egorin, A.; Shlyk, D.; Shi, K.; Hou, X.; Kalmykov, S. Migration Features and Regularities of Heavy Metals Transformation in Fresh and Marine Ecosystems (Peter the Great Bay and Lake Khanka). *Water* **2023**, *15*, 2267. [CrossRef]
43. Bazhenov, A.V. Cesium-137 in the Soils of the Arkhangelsk Region. Ph.D. Thesis, Institute of Geoecology of the RAS, Moscow, Russia, 2001. (In Russian).
44. Cwanek, A.; Łokas, E.; Dinh, C.N.; Zagórski, P.; Singh, S.M.; Szufa, K.; Tomankiewicz, E. 90Sr level and behaviour in the terrestrial environment of Spitsbergen. *J. Radioanal. Nucl. Chem.* **2020**, *327*, 485–494. [CrossRef]
45. Lukoshkova, A.; Yakovlev, E.; Orlov, A. Specific activity and features of vertical migration of strontium-90 in the peat bog of the Murmansk region. *Vestn. Geosci.* **2022**, *329*, 21–25. [CrossRef]
46. Orlov, V.V. *Radiometric Assessment of the Territory of the Arkhangelsk and Novgorod Regions, the North-Western Part of the Komi Republic in Order to Identify and Map Environmentally Unfavorable Areas*; Report AGP-4 on the results of environmental airborne gamma spectrometric survey at a scale of 1:1000000 at the Ecosever site in 1990-1993; State Registration Number 29-90-248/44; Committee of the Russian Federation on Geology: St. Petersburg, Russia, 1993. (In Russian)
47. Glasstone and Sesonske. *Nuclear Reactor Engineering: Reactor Systems Engineering*, 4th ed.; Springer: Berlin, Germany, 1994; ISBN 978-0412985317.
48. Lamarsh, J.R.; Baratta, A.J. *Introduction to Nuclear Engineering*, 3rd ed.; Prentice-Hall: Hoboken, NJ, USA, 2001; ISBN 0-201-82498-1.
49. Stacey, W.M. *Nuclear Reactor Physics*; John Wiley & Sons: Hoboken, NJ, USA, 2001; ISBN 0-471-39127-1.
50. Semenkov, I.N.; Usacheva, A.A.; Miroshnikov, A.Y. Distribution of caesium-137 global fallout in taiga and tundra catenaries of the Ob River basin. *Geol. Ore Depos.* **2015**, *57*, 154–173. [CrossRef]
51. Rakhimova, N.N.; Efremov, I.V.; Gorshenina, E.L. *Migration Abilities of Radionuclides Cs-137 and Sr-90 in Different Types of Soils*; Bulletin of Orenburg State University: Orenburg, Russia, 2015; Volume 10, pp. 412–415.
52. Iglovsky, S.A.; Shvartsman, Y.G.; Bolotov, I.N. *Cryolithozone of the Dvinsko-Mezenskaya Plain and Kanin Peninsula*; NarFU: Arkhangelsk, Russia, 2010; 122p.
53. Klimova, E.B. Influence of macro and microrelief of agricultural lands on 137Cs migration along the soil profile. Ecological safety in agro-industrial complex. *Abstr. J.* **2004**, *4*, 155–158.
54. Barsukov, O.A.; Yazykeev, D.V. *Horizontal and Vertical Migration of 40K, 137Cs, 226Ra, 232Th and 241Am on Cultivated Slope Landscapes of Penza Region of Different Degrees of Steepness; Izvestiya PSPU named after V.G. Belinsky*; Penza State Pedagogical University: Penza, Russia, 2012; Volume 29, pp. 369–374.
55. Korobova, E.M.; Tarasov, O.V.; Romanov, S.L.; Baranchukov, V.S.; Berezkin, V.Y.I.; Modorov, M.V.; Mikhailovskaya, L.N.N.; Lukyanov, V.V. On the distribution of Sr-90 and Cs-137 in elementary landscape-geochemical systems of the East Ural radioactive trace. In Proceedings of the International Scientific and Practical Conference Nuclear Physics Research and Technology in Agriculture, Obninsk, Russia, 16–18 September 2020; pp. 175–177.
56. Matishov, G.G.; Matishov, D.G.; Usyagina, I.S.; Kasatkina, N.E. Multiyear dynamics of radioactive pollution of the Barents-Kara region (1960–2013). *Rep. Acad. Sci.* **2014**, *458*, 473. [CrossRef]
57. Kirchner, G.; Noack, C. Core history and nuclide inventory of the Chernobyl core at the time of accident. *Nucl. Saf.* **1988**, *1*, 29.
58. Stein, A.F.; Draxler, R.R.; Rolph, G.D.; Stunder, B.J.B.; Cohen, M.D.; Ngan, F. NOAA's HYSPLIT Atmospheric Transport and Dispersion Modeling System. *Bull. Am. Meteorol. Soc.* **2015**, *96*, 2059–2077. [CrossRef]
59. Militaryrussia: Website—Moscow. 2009. Available online: http://militaryrussia.ru (accessed on 2 October 2023).